frontiers | Frontiers in Marine Science

TYPE Original Research
PUBLISHED 25 September 2024
DOI 10.3389/fmars.2024.1466216

OPEN ACCESS

EDITED BY
Chaojin Lu,
University of Miami, United States

REVIEWED BY
Chao Liu,
Henan Polytechnic University, China
Ziye Lu,
Southwest Petroleum University, China

*CORRESPONDENCE
Feng Wu
finncug@hotmail.com

RECEIVED 17 July 2024
ACCEPTED 02 September 2024
PUBLISHED 25 September 2024

CITATION
Wu F, Jian Z, Xie X, Bialik OM and Reolid J (2024) Records of Burdigalian sea level and paleoclimate in the Maldives carbonate system. *Front. Mar. Sci.* 11:1466216. doi: 10.3389/fmars.2024.1466216

Records of Burdigalian sea level and paleoclimate in the Maldives carbonate system

Feng Wu[1,2*], Zhimin Jian[1], Xinong Xie[3], Or M. Bialik[4,5] and Jesús Reolid[6]

[1]State Key Laboratory of Marine Geology, Tongji University, Shanghai, China, [2]College of Oceanography, Hohai University, Nanjing, China, [3]College of Marine Science and Technology, China University of Geosciences, Wuhan, China, [4]Institute of Geology and Palaeontology, University of Münster, Münster, Germany, [5]Dr. Moses Strauss Department of Marine Geosciences, The Leon H. Charney School of Marine Sciences, University of Haifa, Haifa, Israel, [6]Departamento de Estratigrafia y Paleontologia, Universidad de Granada, Granada, Spain

Tropical carbonate systems are valuable archives of paleoenvironments, as the carbonate growth is intimately affected by water depth and climatic conditions. Geochemical data from the Burdigalian interval in IODP Site U1468 in the Maldives, northern Indian Ocean, were integrated with sedimentological and paleontological data for a more detailed reconstruction of depositional history. Generally, the Sr/Ca values of slope sediments record highstand progradation in both sequence unit and whole Burdigalian interval, while the absence of higher Sr/Ca ratio close to the sequence boundary during the early Burdigalian could be related to the erosion of deeper-water sediments due to the activity of bottom current. From 20.5 to 19.1 Ma and from 17.9 to 17.2 Ma, nutrient level and productivity were moderately elevated due to the terrigenous input by the intensified South Asian Proto-Monsoon, which also helped cause more reducing conditions in the distal slope. Moreover, increased nutrient level facilitated the growths of calcareous algae and sponges, while it was not favorable for coral development. The elevated nutrient level, higher sea level, and monsoon-induced current contributed to the backstepping of the outer margin during the late Burdigalian. Our study shows an example on how a tropical carbonate platform evolved in response to the interplay of sea-level and paleoclimatic conditions. Findings are expected to be applicable to other tropical carbonate platforms.

KEYWORDS

carbonate system, tropical area, sea level, paleoclimate, Maldives, Burdigalian

1 Introduction

During the Neogene, temperature gradually rose during the Burdigalian, and culminated during the Miocene Climate Optimum (MCO), which was related to an increase in atmosphere CO_2 (Westerhold et al., 2020). In conjunction with the warming, sea level experienced a secular rise from -68 to 60 m due to the shrinking of Antarctic ice sheets (Miller et al., 2020). This occurred coevally to a gradual intensification of both the East Asia Summer Monsoon (EASM) and the South Asian Summer Monsoon (SASM) during this stage (Clift et al., 2014; Betzler et al., 2018). Combined, these shifts likely influenced the development of tropical carbonate platforms across the Indo-Pacific (Betzler et al., 2013; 2016; Wu et al., 2019a).

Carbonate production is closely related to sea level, tectonics, and environmental factors, including temperature, nutrient level, and oxygen level (James, 1997; Betzler et al., 2000; Schlager, 2003; Coletti et al., 2017; Reolid et al., 2017; Michel et al., 2018; Brandano et al., 2019; Wu et al., 2021, 2023). Shallower, warmer, more oligotrophic and oxygenic conditions are generally more favorable for the phototrophic organisms (Hallock and Schlager, 1986; Hallock et al., 1988; Halfar et al., 2006; Montaggioni et al., 2011; Wu et al., 2019b). Platform progradation or backstepping can also occur in response to the combined effect of sea level, tectonics, and environments (Anselmetti et al., 2000; Betzler et al., 2013; 2014; Reolid et al., 2019a; Bialik et al., 2023).

The Maldives platform, located in the central equatorial Indian Ocean, is a tropical carbonate platform isolated from the continents, where nearly a 3 km thick Cenozoic carbonate sequence has accumulated (Figure 1). Seismic investigation of the platforms was interpreted to inform on the long-term Miocene carbonate-platform growth in the Maldives (Belopolsky and Droxler, 2003; Betzler et al., 2013). This platform was tectonically stable during the early Miocene, making it suitable to analyze the influence of sea level and environmental factors on carbonate production (Purdy and Bertram, 1993; Lüdmann et al., 2013). Sedimentological, paleontological and geochemical analysis of the cores, drilled by expedition 359 of the International Ocean Discovery project (IODP), has helped to improve the understanding of the factors controlling platform evolution (e.g., long-term platform-architecture change, platform drowning, drift distribution), reconstruct the monsoon intensity, and reinterpret the record of carbon isotope in carbonate sediments (Betzler et al., 2016; 2018; Lanci et al., 2019; Lindhorst et al., 2019a; Swart et al., 2019; Reolid et al., 2019a; 2020; Bialik et al., 2020; Ling et al., 2021; Lüdmann et al., 2022).

In the Maldives, the Burdigalian is a stage prior to the shallow-water platform drowning (Betzler et al., 2018). Platform progradation towards the Inner Sea was most distinctive during the early Burdigalian (Betzler et al., 2013). Meanwhile, there was an initiation of backstepping in the outer platform margin during the late Burdigalian, which evolved gradually into subsequent stages (Betzler et al., 2018; Reolid et al., 2019a). In this study, we conduct geochemical research [major and trace elements, total organic carbon (TOC), nitrogen isotope of organic matters ($\delta^{15}N_{OM}$)] on the Burdigalian interval of IODP Site U1468 to decode depositional records and reconstruct paleoclimatic conditions. By integrating the

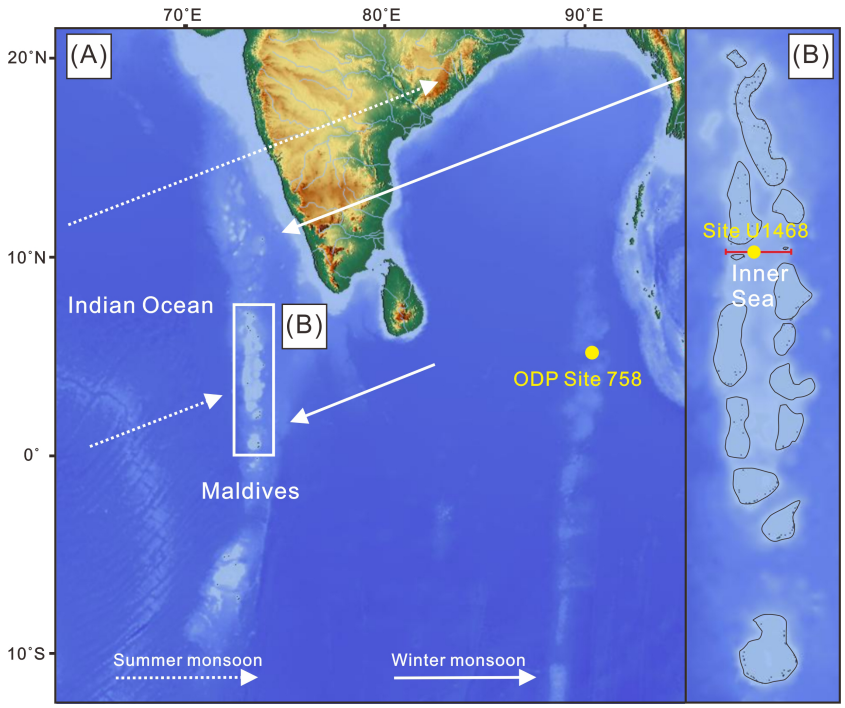

FIGURE 1
(A) Location of the Maldives platform, Indian Ocean. White dashed lines represent summer monsoon, while white solid lines represent winter monsoon. In addition, ODP Site 758 is shown. **(B)** Detailed views of Maldives platform displaying the Inner Sea rimmed by two rows of atolls. The IODP Site U1468 and the seismic profile (red line) crossing this site are also shown.

geochemical data with sedimentological and paleontological data, we analyze the Burdigalian platform evolution in detail and uncover the impact of sea level and paleoclimate on the platform evolution during this stage.

2 Geological setting

The isolated Maldives archipelago in the equatorial Indian Ocean is a carbonate platform initiating on the Early Paleogene Chagos-Laccadives volcanic ridge (Aubert and Droxler, 1992; Purdy and Bertram, 1993). A double row of atolls arranged in N-S direction encloses the Inner Sea, which has a water depth ranging from 300 to 550 m (Betzler et al., 2018). The oceanward slopes are generally steep until the water depth of 2000 m (Betzler et al., 2018). During the Early Eocene, carbonate production occurred on the topographic highs in the Maldives area (Aubert and Droxler, 1996). Neritic carbonate bank sediments accumulated on the shoulders of the graben structure from Eocene to Oligocene under conditions of relative sea level rise (Aubert and Droxler, 1996; Belopolsky and Droxler, 2003). During the Oligocene, the platform developed elevated marginal rims and a depressed inner lagoon (Aubert and Droxler, 1996; Betzler et al., 2016). Above the Oligocene-Miocene boundary, a total of 11 sequence boundaries (i.e., PS1-PS11) help identify 11 platform sequences (i.e., ps1-ps11) before 12.9 Ma (Betzler et al., 2018). Sequence ps1 and ps3 are mainly characterized by aggradation, while ps2 and ps4 are mainly characterized by distinct eastward progradation to the Inner Sea. Aggradation was present again in ps5, ps6, and ps7, and the eastward progradation was relatively most important in ps6 among these three sequences. Moreover, a backstepping started to occur in ps6 in the outer margin close to the open Indian Ocean. Pronounced progradation developed in ps8-ps11 (Betzler et al., 2013, 2018). Sediments progradation and aggradation during the Early Miocene gradually modified a gentle ramp into a steep-flanked platform (Betzler et al., 2013; 2016). Around 12.9 Ma, there was a partial drowning event in the platform, which was accompanied by thick drift deposits in the Inner Sea (Betzler et al., 2016; Lüdmann et al., 2018; Reolid et al., 2019b). The sequence boundary around 12.9 Ma separates the underlying carbonate bank from the overlying drift deposits. There are 10 drift sequences in total. Drift deposits were funneled through passages between the remaining banks, and drift deposition center varied gradually eastward. Monsoon-induced current was the most important factor controlling the platform evolution after 12.9 Ma (Betzler et al., 2016; 2018). Skeletal analysis indicated that planktonic and benthic foraminifera are the most important components in the carbonate banks and drifts (Reolid et al., 2019a, 2019b).

3 Materials and methods

The samples from IODP site U1468 (4° 55.98'N, 73° 4.28'E) were collected and tested to obtain elemental concentration, organic matter abundance, and nitrogen isotopes. Major and minor elements were analyzed using an inductively coupled plasma atomic emission spectrometer (ICP-AES) and an inductively coupled plasma emission mass spectrometer (ICP-MS), respectively, at the State Key Laboratory of Marine Geology in Tongji University. Testing precision based on duplicates was better than 2% for all the samples. The total organic carbon (TOC) and nitrogen isotope testing were conducted at the State Key Laboratory of Biogeology and Environmental Geology (BGEG), China University of Geosciences. HCL (50%) was utilized to decarbonate sample powders. Deionized water was used to rinse the insoluble residues until neutral, and the residues were dried at 50°C overnight and powered again. TOC was measured by a 902T C-S analyzer at the BGEG. Analytical precision was better than 0.1% for all samples. The dry powders were weighted into tin capsules for nitrogen isotope testing and combusted at 960°C. The evolved N2 was analyzed using a continuous-flow Delta V Advantage IRMS. Nitrogen isotope results are reported using standard δ notation as deviations from the $\delta^{15}N$ composition of atmospheric N_2 (0‰). Analytical precision was better than 0.3‰. The abundance of productivity and nutrient elements (i.e., Cd, Ni, Ba) is normalized to both Ti and Al, in order to better show the changes in productivity and nutrient level during the Burdigalian. Al normalization was not conducted on the samples with Al/Ti ratio values higher than 21, as Al-excess is possibly recorded in these samples and Al normalization is not suitable for these samples (Murray and Leinen, 1996). Moreover, the curve of oxygen isotopic record from IODP Site U1468 is similar to the global trends, which indicates limited diagenetic influence (Bialik et al., 2020). This denotes that the elements can be used to trace chemical changes in seawater.

Seismic data across the Maldives platform are obtained after Reolid et al. (2019a) in order to show the characteristics of Burdigalian sequences (Figure 2). As the sequence boundary PS3 is amalgamated with PS2 around Site U1468 at seismic scale (Betzler et al., 2018), we combine the platform sequence ps2, ps3, and ps4 at Site U1468 to obtain a better correlation between core and seismic profile data. The age model of Site U1468 follows Spezzaferri et al. (2022), which provided an improved version with detailed identification of planktonic foraminifera, calcareous nannofossils, and benthic foraminifera. Moreover, the identified benthic foraminifera data are also utilized in this study to better reflect the response of carbonate-platform evolution to sea level and paleoclimate.

4 Results

The Sr/Ca ratio varies between 0.0018 and 0.0032 (ppm/ppm, this is the same for following elemental ratios). It increases upwards in ps5, ps6, and the lower part of ps2-ps4, while there is not obvious change in the long-term Sr/Ca values in the whole Burdigalian interval (Figure 3). For U/Ti, V/Ti, Mo/Ti, Cd/Ti, Cd/Al, Ni/Ti, Ni/Al, Ba/Ti, Ba/Al, Fe/Al ratios, their values are generally higher in ps2-ps4 (with averages of 0.306, 0.428, 0.049, 0.010, 0.0006, 1.729, 0.075, 0.137, 0.006, 0.607, respectively), and in the lower part of ps6 (with averages of 0.261, 0.456, 0.117, 0.011, 0.0007, 1.542, 0.110, 0.146, 0.008, 1.019, respectively), while they are generally lower in ps5 (with averages of 0.151, 0.236, 0.050, 0.006, 0.0003, 1.240, 0.062,

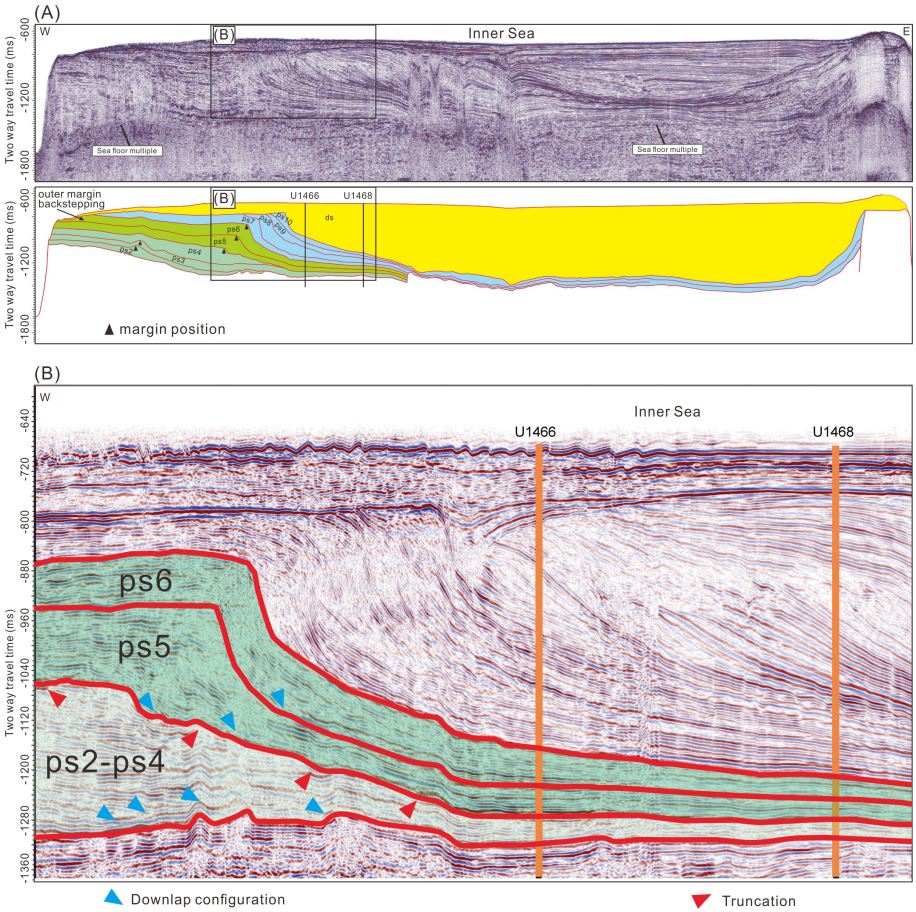

FIGURE 2
(A) Seismic profile across the Maldives Inner Sea (see Figure 1B for the profile location) with red lines showing the platform sequence units (ps1 to ps10) (after Betzler et al., 2018). Light green (ps2-ps4) and dark green (ps5-ps6) are the Burdigalian intervals. **(B)** Seismic profile from platform to the Inner Sea in the western Maldives (after Reolid et al., 2019a). Terminations (downlap and truncation) of the seismic reflectors and positions of Sites U1466 and U1468 are shown. Location of this profile is shown in **(A)**.

0.101, 0.005, 0.148, respectively) and in the upper part of ps6 (with averages of 0.093, 0.204, 0.020, 0.005, 0.0003, 0.776, 0.048, 0.082, 0.005, 0.556, respectively) (Figure 3).

The TOC values are highest in ps2-ps4 with an average of 0.29, followed by those in ps6 with an average of 0.15, and subsequently by those in ps5 with an average of 0.14 (Figure 3). The $\delta^{15}N_{OM}$ values are highest in ps5 with an average of 1.23‰, followed by those in ps6 with an average of 1.05‰, and subsequently by those in ps2-ps4 with an average of 0.91‰ (Figure 3).

5 Discussion

5.1 Records of sea level and current during the Burdigalian

Previous studies on carbonate platforms have shown that carbon isotope ($\delta^{13}C$) and Sr/Ca are possibly useful indexes, as platform-top sediments dominantly consist of aragonite characterized by higher $\delta^{13}C$ and Sr/Ca values while pelagic sediments dominantly consist of low-Mg calcite characterized by lower $\delta^{13}C$ and Sr/Ca values (Swart and Eberli, 2005; Swart, 2008; Bialik et al., 2020, 2024; Alonso-Garcia et al., 2024). In Site U1468, Sr/Ca values show an upward increase in ps5, ps6, and the lower part of ps2-ps4 (Figure 4A), suggesting increases in shallow-water components upwards in each sequence. These are similarly interpreted here to represent "highstand shedding" from the platform top (Schlager et al., 1994). This agrees well with the sediment architecture recorded in the seismic profile, which shows the gradual migration of platform inner margin towards the Inner Sea (Figure 2B). In euphotic platforms, "highstand shedding" is considered indicative of sea level controls. When platform top is flooded in the highstand, shallow-water carbonate factory on the platform top is active to produce and shed abundant sediments to the slope. As records of sea-level variations, "highstand shedding" has been reported in many other euphotic platforms, such as Great Bahama Bank (Boardman et al., 1986; Eberli et al., 2001), although the pattern is somewhat different in mesophotic platforms (Bialik et al., 2024). Furthermore, there is a longer-term (5Ma scale) increase in Sr/Ca values from ps2 to ps6 (Figure 4A), which is in line with the longer-term increase in $\delta^{13}C$ values from the Burdigalian to the early Langhian in Site U1468 (Swart et al.,

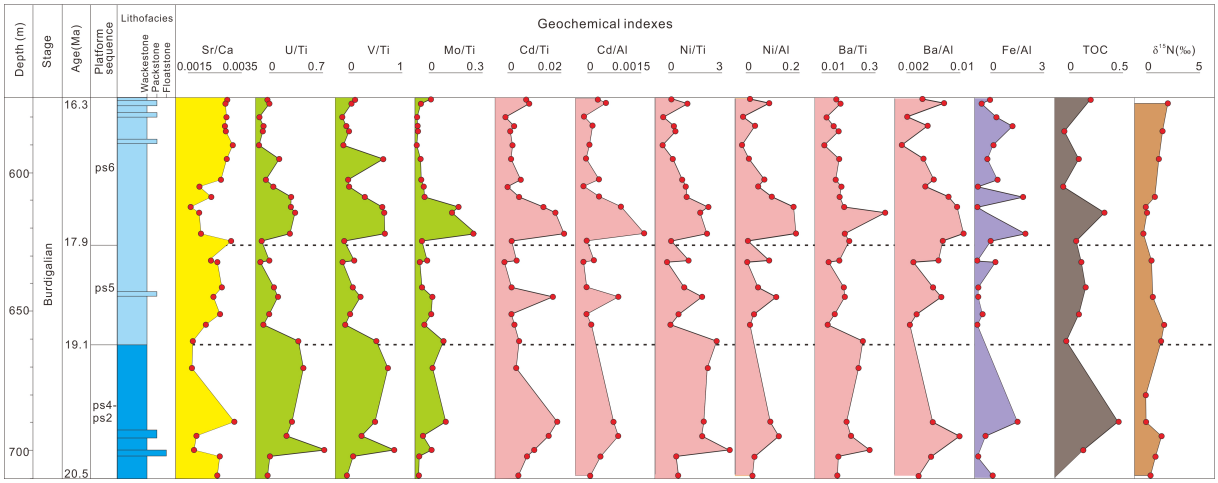

FIGURE 3
Integrated data of Burdigalian interval in Site U1468. (1) Depth (m); (2) Stage; (3) Age (Ma); (4) Platform sequence (Reolid et al., 2019a); (5) Lithofacies (Reolid et al., 2019a); (6) Geochemical indexes, including Sr/Ca, U/Ti, V/Ti, Mo/Ti, Cd/Ti, Cd/Al, Ni/Ti, Ni/Al, Ba/Ti, Ba/Al, Fe/Al, TOC, and $\delta^{15}N_{OM}$.

2019). Both these two proxies indicate longer-term progradation from ps2 to ps6. In the seismic profile, the platform margin migrated towards the Inner Sea from ps2 to ps6, which is in line with the geochemical signals. This was the response to the secular change in sea level from 20.5 to 16.3 Ma (Figure 4B).

There is no increase in Sr/Ca ratio in the upper part of ps2-ps4 (Figure 4A). This could result from heavy erosion of the upper ps4. Different to the continuous stacking in the platform top from ps2-ps4 to ps6, the thickness of ps2-ps4 in the slope environment was heavily reduced. The seismic profile shows that there are truncations on the upper ps4 (Figure 2B), which indicates the occurrence of erosion. Erosion of platform sediments in the shallower waters occurred when part of the platform top was likely exposed during low sea-level conditions (Figure 4B). Skeletal assemblage analysis from Site U1468 indicates that ps2-ps4 is characterized by planktonic foraminifera, benthic foraminifera, echinoids, and mollusks (Reolid et al., 2019a; Spezzaferri et al., 2022). Middle-shallow-water benthic foraminiferal species occurred in the lower part of ps2-ps4, and shallow-water benthic foraminiferal species occurred in the upper part of ps2-ps4 (Figure 4A; Spezzaferri et al., 2022), suggesting that these shallower species arrived at the slope after certain transport from 20.5 to 19.1 Ma in response to the sea level lowering. Sea-level fall was an important factor limiting the platform-top carbonate production, which would export relatively less sediments to the slope and cause the formation of thin slope succession. Despite this, sea level itself would not cause erosion in the slope. The water depth at Site U1468, reconstructed from benthic and planktonic foraminiferal assemblage, was more than 350 m (Spezzaferri et al., 2022), which suggests that the direct meteoric dissolution, if any, would have been limited to the platform top and uppermost part of the slope. This also hints that there could be another factor influencing the erosion of deeper-water carbonate sediments.

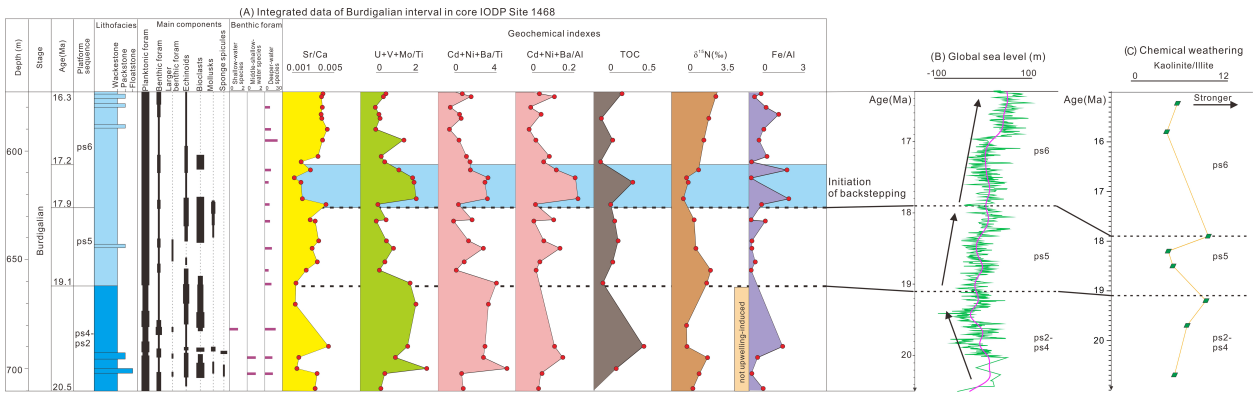

FIGURE 4
(A) Integrated data of Burdigalian interval in Site U1468: (1) Depth (m); (2) Stage; (3) Age (Ma); (4) Platform sequence (Reolid et al., 2019a); (5) Lithofacies (Reolid et al., 2019a); (6) Main components (Reolid et al., 2019a); (7) Benthic foraminifera (Spezzaferri et al., 2022); (8) Geochemical indexes (Sr/Ca, U+V+Mo/Ti, Cd+Ni+Ba/Ti, Cd+Ni+Ba/Al, TOC, $\delta^{15}N_{OM}$, and Fe/Al). **(B)** Global sea level change during the Burdigalian (Miller et al., 2020). **(C)** Chemical weathering variation recorded in ODP Site 758 during the Burdigalian (Ali et al., 2021).

In such a deep-water setting, bottom current was a possible factor inducing the erosion, which was widely reported in other carbonate platforms (Anselmetti et al., 2000) as well as in the younger intervals of the Maldives platform (Betzler et al., 2016, 2018). Planktonic and benthic foraminiferal assemblages (i.e., abundant planktonic foraminifera from the surface mixed layer to the subthermocline and benthic species *Cibicides wuellerstorfi*) and their poor to moderate preservation state in ps2-ps4 interval of Site U1468 suggest that these fossils could have been transported by relatively stronger bottom current (Spezzaferri et al., 2022). There are records of other carbonate platforms elsewhere that show intensification of bottom currents and concomitant erosion of the slopes during periods of low sea level (e.g., Great Bahama Bank, Anselmetti et al., 2000; Principaud et al., 2016; Wunsch et al., 2018), which is similar to the scenario during the deposition of ps2-ps4 from 20.5 to 19.1 Ma in the Maldives platform (Figure 4B). Although bottom currents were indeed globally important after the middle Miocene, which fundamentally modified the architecture of carbonate platforms around the world (Betzler and Eberli, 2019), there are also some reports about the activity of bottom current during the Burdigalian. In Cyprus, there are thick carbonate contourite deposits from the Eocene to the Middle Miocene, and the coarse-grained contourites were deposited during the Burdigalian when the global sea level was lower (Hernández-Molina et al., 2022). Similar bottom-current activity was also registered in the Chatham Rise, New Zealand (Carter et al., 2004; Steinbrink et al., 2020). These examples signify that the bottom current was also relevant in shaping carbonate platforms when the ice sheet developed only in East Antarctica (Westerhold et al., 2020). From 19.1 Ma to 14 Ma, there was a rough increase in the preservation state of planktonic and benthic foraminifera in the Maldives (Spezzaferri et al., 2022), possibly hinting that the bottom-current influence became weaker when the polar ice sheet retreated, and the global sea level gradually rose. The relatively more continuously distributed slope successions from ps5 to ps10 also support the gradual weaker impact of erosion from the bottom current.

5.2 Records of paleoclimate during the Burdigalian

Among the platform sequences, ps2-ps4 is generally characterized by higher values of U/Ti, V/Ti, Mo/Ti, and (U+V+Mo)/Ti ratios (Figures 3, 4A). The U/Ti, V/Ti, Mo/Ti, and also (U+V+Mo)/Ti ratios are redox-related, and their higher values can indicate a more reducing environment (Tribovillard et al., 2006). Therefore, the consistently higher values of these ratios indicate that the distal slope from 20.5 to 19.1 Ma was relatively more reducing during the Burdigalian. Research on the underlying sapropel intervals in the Maldives suggested that anoxic conditions caused by highly restricted circulation protected the organic matter from oxidation and decay when the global sea level was generally low (Swart et al., 2019). As the intervals of ps2-ps4 were accumulated in the relatively lower sea-level settings (Figure 4B), it is possible that some restriction could have contributed to the formation of reducing conditions. Despite this, according to the discussion in the previous section, there was a stronger circulation in the slope environment. It is deduced that the reducing conditions from 20.5 to 19.1 Ma was also related to another factor. In company with higher values of U/Ti, V/Ti, Mo/Ti, and (U+V+Mo)/Ti ratios, higher values of Cd/Ti, Ni/Ti, Ba/Ti, and (Cd+Ni+Ba)/Ti ratios also occur in the ps2-ps4 interval (Figures 3, 4A), indicating that the productivity and nutrient level from 20.5 to 19.1 Ma was also elevated (Tribovillard et al., 2006). Moreover, TOC is higher, which is in line with the Cd/Ti, Ni/Ti, Ba/Ti, and (Cd+Ni+Ba)/Ti values (Figures 3, 4A). In many environments elsewhere, higher nutrient availability produces plentiful organic matters and the decay of organic matters consumes oxygen in the seawater, which helps preserve the remains of organic matters (Tribovillard et al., 2006; Sajid et al., 2020; Wang et al., 2022). Thus, it is possible that higher nutrient level and productivity also facilitated the formation of reducing condition from 20.5 to 19.1 Ma in the distal-slope environment. Similar to ps2-ps4, the lower part of ps6 is also generally characterized by higher values of U/Ti, V/Ti, Mo/Ti, and (U+V+Mo)/Ti ratios (Figures 3, 4A), indicating that the depositional environment from 17.9 to 17.2 Ma was also more reducing. Meanwhile, the lower part of ps6 is also characterized by higher values of Cd/Ti, Cd/Al, Ni/Ti, Ni/Al, Ba/Ti, Ba/Al, (Cd+Ni+Ba)/Ti, (Cd+Ni+Ba)/Al, and TOC (Figures 3, 4A), which also suggests that the moderately reducing environment could be linked to the higher nutrient level and productivity. In contrast, ps5 is characterized by lower values of U/Ti, V/Ti, Mo/Ti, (U+V+Mo)/Ti, Cd/Ti, Cd/Al, Ni/Ti, Ni/Al, Ba/Ti, Ba/Al, (Cd+Ni+Ba)/Ti, (Cd+Ni+Ba)/Al, and TOC (Figures 3, 4A). This could indicate that the lower nutrient and productivity promoted fewer production of organic matters and thus did not favor the formation of a more reducing environment. According to Miller et al. (2020), the period corresponding to ps5 was marked by sea levels lower than that of ps6. If we assume that restriction was the main factor responsible for the formation of reducing condition and rich organic matters, the lower sea levels from 19.1 to 17.9 Ma would result in a more intense restriction than that from 17.9 to 17.2 Ma, which would produce more reducing condition. However, this assumption is in contradictory to the fact that the condition from 17.9 to 17.2 Ma was more reducing than from 19.1 to 17.9 Ma (Figure 4A). This contradiction and the consistency between productivity and redox condition strongly indicate that productivity has also played an important role in shaping the redox condition during the Burdigalian in the distal-slope environment.

For the organic matters in the Burdigalian interval, nitrogen isotope analysis yielded $\delta^{15}N_{OM}$ values between 0.36 and 1.89‰ (Figure 4A). Previous study in the younger interval of the Maldives has indicated that the upwelled nitrate is characterized by a strong denitrification with nitrogen isotopic values of the upwelling-related organic matters higher than 4‰ (Ling et al., 2021), which was also recorded elsewhere (Algeo et al., 2008). The lower $\delta^{15}N_{OM}$ values in the Burdigalian interval suggests that upwelled nitrate was not the major source of nitrogen in producing the organic matters in the Maldives. The nutrients could be sourced from the terrigenous input. Dust could be a potential source, as the Maldives were an isolated platform during the Miocene. Nitrogen in the dust is typically characterized by isotopic values close to 0 (Knapp et al., 2010), which was more consistent with the $\delta^{15}N_{OM}$ values in the organic matters in the Burdigalian interval. Fe/Al ratio has been considered as a valid proxy for dust in the younger intervals in the Maldives and

Bahama platforms (Bunzel et al., 2017; Lindhorst et al., 2019b). The long-term change in Fe/Al ratio is generally in line with those in (Cd+Ni+Ba)/Ti and (Cd+Ni+Ba)/Al, suggesting a link between the dust and nutrients (Figure 4A). In addition, there is a general correspondence between lower $\delta^{15}N_{OM}$ values and higher Fe/Al ratio values, possibly suggesting that increased dust influence. The dust input could be related with the South Asian Proto-Monsoon, which delivered the terrigenous material to the Maldives platform (Betzler et al., 2016). Besides, in the Maldives, the progradation towards the Inner Sea occurred obviously in the western bank during the formation of ps2-ps6, while it was much less apparent in the eastern bank (Betzler et al., 2013). Progradation in the western bank was more important in ps2-ps4 and ps6 than in ps5 (Betzler et al., 2013). The summer proto-monsoon was likely stronger during the formation of ps2-ps4 and ps6, as the strong summer proto-monsoon would promote the development of preferential progradation towards the leeward side (Betzler et al., 2016). The stronger summer proto-monsoon could have caused a slight increase in precipitation in the South Aisa, which facilitated the weathering process in the South Asia. The long-term chemical weathering records from IODP Site 758, which is located in the northern Indian Ocean and close to the Maldives platform (Figure 1A), indicate that the period of 19.1-17.9 Ma was characterized by weaker chemical weathering compared to the periods of 20.5-19.1 Ma and 17.9-15 Ma (Figure 4C) (Ali et al., 2021). The more intense chemical weathering contributed to a moderate increase in delivery of nutrients into the northern Indian Oceans, which was common elsewhere (Clift et al., 2014; Li et al., 2022).

The elevated nutrient level could also have some effect on the platform growth. The occurrence of calcareous algae is mainly restricted to ps2-ps4 and the lower part of ps6 in Site U1466 (Reolid et al., 2019a). This indicates the effect of elevated nutrient level, as the coralline algae mainly thrive in slightly mesotrophic conditions (Halfar et al., 2006). Meanwhile, the presence of sponge spicules in ps2-ps4 interval in Site U1468 could also be related to the higher nutrient level (Figure 4A), as the sponge spicules usually occurred in the elevated trophic conditions elsewhere (Perea-Blázquez et al., 2012). For ps6, it is indicated in the seismic profile that backstepping started to occur in the outer margin (Figure 2A). The eustatic sea level gradually rose and culminated around 16.4 Ma (Figure 4B, Miller et al., 2020), and such a rise in sea level would have some impact on the shrink of the carbonate platform, as corals in the platform top generally tend to thrive in the shallower waters (Schlager, 2003). Moreover, corals prefer to thrive in oligotrophic waters and tend to be suppressed in elevated nutrient level (Hallock and Schlager, 1986; Halfar et al., 2006). Thus, the higher nutrient level between 17.9 and 17.2 Ma could also have contributed to damage the coral growths at the platform margin. Similar decline in corals and increase in coralline algae occurred in the global scale during the late Burdigalian and Serravallian, which was linked to elevated nutrient level caused by generally increased land-weathering rates and nutrient input (Halfar and Mutti, 2005). In addition, the proto-monsoon would also cause currents on the platform top, which swept the newly produced carbonate sediments into the Inner Sea. The settling of coral larvae at the platform margin would also be threatened by the monsoon-induced currents (Ling et al., 2021). Therefore, it is deduced that the backstepping during the formation of ps6 was the coupled results of rising sea level and intensified summer proto-monsoon, which caused elevation in nutrient level and current speed. The absence of corals facilitated the erosion at the marginal zone and the transport of sediments across the platform top into the slope area (Reolid et al., 2019a). After 17.2 Ma, the nutrient level declined, but the sea level became higher (Figure 4B). Such a higher sea level increased the potential of backstepping in the outer margin. Proto-monsoon was possibly weaker, but the currents still contributed to the backstepping, which evolved in the following stage.

6 Conclusions

Based on the geochemical, sedimentological, and paleontological data from IODP Site U1468, we analyze the Burdigalian evolution of the Maldives platform. "Highstand shedding" in the sequence unit was recorded in the Sr/Ca values in the distal slope. Erosion occurred especially in the lower sea-level settings during the early Burdigalian, which was possibly caused by meteoric influence in the shallower waters and bottom currents in the deeper waters. In addition to the restriction effect, higher nutrient level and productivity have also contributed to the occurrence of more reducing conditions and more organic matters from 20.5 to 19.1 Ma and from 17.9 to 17.2 Ma. The higher nutrient availability and productivity were linked to the terrigenous dust and weathering inputs due to the intensification of South Asian Proto-Monsoon. Moreover, the elevated nutrient level had some positive effect on the growth of calcareous algae and sponges, while it was possibly not favorable for coral development at the platform margin. Coupled with raised sea level and monsoon-induced current, the moderately elevated nutrient level caused the backstepping of the outer margin during the late Burdigalian. These results show how the regional and global factors modified the growth of a carbonate platform in the tropical area.

Data availability statement

The original contributions presented in the study are included in the article/Supplementary Material, further inquiries can be directed to the corresponding author.

Author contributions

FW: Conceptualization, Data curation, Formal analysis, Funding acquisition, Investigation, Methodology, Resources, Writing – original draft, Writing – review & editing. ZJ: Methodology, Conceptualization, Formal analysis, Investigation, Supervision, Writing – review & editing. XX: Conceptualization, Formal analysis, Funding acquisition, Investigation, Methodology,

Project administration, Resources, Supervision, Validation, Writing – review & editing. OB: Methodology, Conceptualization, Investigation, Writing – review & editing. JR: Conceptualization, Formal analysis, Funding acquisition, Investigation, Methodology, Project administration, Resources, Validation, Writing – review & editing.

Funding

The author(s) declare that financial support was received for the research, authorship, and/or publication of this article. This study was supported by the National Natural Science Foundation of China (42130408; 42106058). JR thanks the Spanish Ministry of Science and Innovation (MCIN) for funding through the Ramón y Cajal Project RYC2021-034362-I (MCIN/AEI/10.13039/501100011033 and Next Generation EU/PRTR).

Acknowledgments

The authors would like to thank the IODP for providing samples of Site U1468 from the Maldives.

Conflict of interest

The authors declare that the research was conducted in the absence of any commercial or financial relationships that could be construed as a potential conflict of interest.

Publisher's note

Supplementary material

The Supplementary Material for this article can be found online at: https://www.frontiersin.org/articles/10.3389/fmars.2024.1466216/full#supplementary-material

References

Algeo, T., Rowe, H., Hower, J. C., Schwark, L., Herrmann, A., and Heckel, P. (2008). Changes in ocean denitrification during Late Carboniferous glacial–interglacial cycles. *Nat. Geosciences* 1, 709–714. doi: 10.1038/ngeo307

Ali, S., Hathorne, E. C., and Frank, M. (2021). Persistent provenance of South Asian monsoon-induced silicate weathering over the past 27 million years. *Paleoceanography Paleoclimatology* 36, 1–15. doi: 10.1029/2020PA003909

Alonso-Garcia, M., Reolid, J., Jimenez-Espejo, F. J., Bialik, O. M., Alvarez Zarikian, C. A., Laya, J. C., et al. (2024). Sea-level and monsoonal control on the Maldives carbonate platform (Indian Ocean) over the last 1.3 million years. *Climate Past* 20, 547–571. doi: 10.5194/cp-20-547-2024

Anselmetti, F. S., Eberli, G. P., and Ding, Z. D. (2000). From the Great Bahama Bank into the Straits of Florida: A margin architecture controlled by sea-level fluctuations and ocean currents. *Geological Soc. America Bull.* 112, 829–844. doi: 10.1130/0016-7606(2000)112<829:FTGBBI>2.0.CO;2

Aubert, O., and Droxler, A. W. (1992). General Cenozoic evolution of the Maldives carbonate system (equatorial Indian Ocean). *Bull. Des. centres recherches exploration-Production Elf-Aquitaine* 16, 113–136.

Aubert, O., and Droxler, A. (1996). Seismic stratigraphy and depositional signatures of the Maldive carbonate system (Indian Ocean). *Mar. Petroleum Geology* 13, 503–536. doi: 10.1016/0264-8172(96)00008-6

Belopolsky, A., and Droxler, A. (2003). Imaging Tertiary carbonate system—the Maldives, Indian Ocean: insights into carbonate sequence interpretation. *Leading Edge* 22, 646–652. doi: 10.1190/1.1599690

Betzler, C., and Eberli, G. P. (2019). Miocene start of modern carbonate platforms. *Geology* 47, 771–775. doi: 10.1130/G45994.1

Betzler, C., Eberli, G. P., Kroon, D., Wright, J. D., Swart, P. K., Nath, B. N., et al. (2016). The abrupt onset of the modern South Asian Monsoon winds. *Sci. Rep.* 6, 1–10. doi: 10.1038/srep29838

Betzler, C., Eberli, G. P., Lüdmann, T., Reolid, J., Kroon, D., Reijmer, J. J. G., et al. (2018). Refinement of Miocene sea level and monsoon events from the sedimentary archive of the Maldives (Indian Ocean). *Prog. Earth Planetary Sci.* 5, 1–18. doi: 10.1186/s40645-018-0165-x

Betzler, C., Fuerstenau, J., Lüdmann, T., Huebscher, C., Lindhorst, S., Paul, A., et al. (2013). Sea-level and ocean-current control on carbonate-platform growth, Maldives, Indian Ocean. *Basin Res.* 25, 172–196. doi: 10.1111/j.1365-2117.2012.00554.x

Betzler, C., Kroon, D., and Reijmer, J. J. G. (2000). Synchroneity of major Late Neogene sea level fluctuations and paleoceanographically controlled changes as recorded by two carbonate platforms. *Paleoceanography* 15, 722–730. doi: 10.1029/1999PA000481

Betzler, C., Lindhorst, S., Eberli, G. P., Lüdmann, T., Möbius, J., Ludwig, J., et al. (2014). Periplatform drift: The combined result of contour current and off-bank transport along carbonate platforms. *Geology* 42, 871–874. doi: 10.1130/G35900.1

Bialik, O. M., Betzler, C., Braga, J. C., Reijmer, J. J., Reolid, J., and Lindhorst, S. (2024). Changes in mesophotic carbonate-platform export across the end of the last glacial cycle (Saya de Malha Bank, western Indian Ocean). *Depositional Rec.* 1, 1–24. doi: 10.1002/dep2.v10.3

Bialik, O. M., Coletti, G., Mariani, L., Commissario, L., Desbiolles, F., and Meroni, A. N. (2023). Availability and type of energy regulate the global distribution of neritic carbonates. *Sci. Rep.* 13, 19687. doi: 10.1038/s41598-023-47029-4

Bialik, O. M., Reolid, J., Betzler, C., Eberli, G. P., and Waldmann, N. D. (2020). Source shifts to periplatform deposits during the early to middle Miocene in response to climatic and oceanographic forcing, Maldives, western Indian Ocean. *Palaeogeography palaeoclimatology Palaeoecol.* 559, 109969. doi: 10.1016/j.palaeo.2020.109969

Boardman, M. R., Neumann, A. C., Baker, P. A., Dulin, L. A., Kenter, R. J., Hunter, G. E., et al. (1986). Banktop responses to Quaternary fluctuations in sea level recorded in periplatform sediments. *Geology* 14, 28–31. doi: 10.1130/0091-7613(1986)14<28:BRTQFI>2.0.CO;2

Brandano, M., Tomassetti, L., Mateu-Vicens, G., and Gaglianone, G. (2019). The seagrass skeletal assemblage from modern to fossil and from tropical to temperate: Insight from Maldivian and Mediterranean examples. *Sedimentology* 66, 2268–2296. doi: 10.1111/sed.12589

Bunzel, D., Schmiedl, G., Lindhorst, S., Mackensen, A., Reolid, J., Romahn, S., et al. (2017). A multi-proxy analysis of Late Quaternary ocean and climate variability for the Maldives, Inner Sea. *Climate Past* 13, 1791–1813. doi: 10.5194/cp-13-1791-2017, 2017

Carter, L., Carter, R. M., and McCave, I. N. (2004). Evolution of the sedimentary system beneath the deep Pacific inflow off eastern New Zealand. *Mar. Geology* 205, 9–27. doi: 10.1016/S0025-3227(04)00016-7

Clift, P. D., Wan, S., and Blusztajn, J. (2014). Reconstructing chemical weathering, physical erosion and monsoon intensity since 25 Ma in the northern South China Sea: A review of competing proxies. *Earth-Science Rev.* 130, 86–102. doi: 10.1016/j.earscirev.2014.01.002

Coletti, G., El Kateb, A., Basso, D., Cavallo, A., and Spezzaferri, S. (2017). Nutrient influence on fossil carbonate factories: Evidence from SEDEX extractions on Burdigalian limestones (Miocene, NW Italy and S France). *Palaeogeography Palaeoclimatology Palaeoecol.* 475, 80–92. doi: 10.1016/j.palaeo.2017.03.005

Eberli, G. P., Anselmetti, F. S., Kenter, J. A. M., Mcneill, D. F., and Melim, L. A. (2001). "Calibration of seismic sequence stratigraphy with cores and logs," in *Subsurface geology of a prograding carbonate platform margin, Great Bahama Bank:*

results of the Bahamas drilling project: SEPM (Society for Sedimentary Geology), vol. 70 . Ed. R. N. Ginsburg (Tulsa, USA: Special Publications), 241–265.

Halfar, J., Godinez-Orta, L., Mutti, M., Valdez-Holguin, J. E., and Borges, J. M. (2006). Carbonates calibrated against oceanographic parameters along a latitudinal transect in the Gulf of California, Mexico. *Sedimentology* 53, 297–320. doi: 10.1111/j.1365-3091.2005.00766.x

Halfar, J., and Mutti, M. (2005). Global dominance of coralline red-algal facies: a response to Miocene oceanographic events. *Geology* 33, 481–484. doi: 10.1130/G21462.1

Hallock, P., Hine, A. C., Vargo, G. A., Elrod, J. A., and Jaap, W. C. (1988). Platforms of the Nicaraguan Rise-examples of the sensitivity of carbonate sedimentation to excess trophic resources. *Geology* 16, 1104–1107. doi: 10.1130/0091-7613(1988)016<1104:POTNRE>2.3.CO;2

Hallock, P., and Schlager, W. (1986). Nutrient excess and the demise of coral reefs and carbonate platforms. *Palaios* 1, 389–398. doi: 10.2307/3514476

Hernández-Molina, F. J., Hüneke, H., Rodríguez-Tovar, F. J., Ng, Z. L., Llave, E., Mena, A., et al. (2022). Eocene to middle Miocene contourite deposits in Cyprus: A record of Indian Gateway evolution. *Global Planetary Change* 219, 103983. doi: 10.1016/j.gloplacha.2022.103983

James, N. P. (1997). "The cool-water carbonate depositional realm," in *Cool-Water Carbonates*. Eds. N. P. James and M. J. Clarke (Society for Sedimentary Geology (SEPM) Special Publications, Society for Sedimentary Geology (SEPM, Tulsa, USA), 1–20.

Knapp, A. N., Hastings, M. G., Sigman, D. M., Lipschultz, F., and Galloway, J. N. (2010). The flux and isotopic composition of reduced and total nitrogen in Bermuda rain. *Mar. Chem.* 120, 83–89. doi: 10.1016/j.marchem.2008.08.007

Lanci, L., Zanella, E., Jovane, L., Galeotti, S., Alonso-García, M., Alvarez-Zarikian, C. A., et al. (2019). Magnetic properties of early Pliocene sediments from IODP Site U1467 (Maldives platform) reveal changes in the monsoon system. *Palaeogeography Palaeoclimatology Palaeoecol.* 533, 109283. doi: 10.1016/j.palaeo.2019.109283

Li, M., Ouyang, T., Zhu, Z., Tian, C., Peng, S., Zhong, H., et al. (2022). Reconstruction of chemical weathering Intensity and Asian Summer Monsoon Evolution in the Red River Basin over the past 36 kyr. *Paleoceanography Paleoclimatology* 37, e2021PA004397. doi: 10.1029/2021PA004397

Lindhorst, S., Betzler, C., and Kroon, D. (2019a). Wind variability over the northern Indian Ocean during the past 4 million years - Insights from coarse aeolian dust (IODP exp. 359, site U1467, Maldives). *Palaeogeography Palaeoclimatology Palaeoecol.* 536, 109371. doi: 10.1016/j.palaeo.2019.109371

Lindhorst, S., Betzler, C., Wunsch, M., Ludmann, T., and Kuhn, G. (2019b). Carbonate drifts as marine archives of aeolian dust (Santaren Channel, Bahamas). *Sedimentology* 66, 1–24. doi: 10.1111/sed.2019.66.issue-4

Ling, A., Eberli, G. P., Swart, P. K., Reolid, J., Stainbank, S., Ruggeberg, A., et al. (2021). Middle Miocene platform drowning in the Maldives associated with monsoon-related intensification of currents. *Palaeogeography Palaeoclimatology Palaeoecol.* 567, 110275. doi: 10.1016/j.palaeo.2021.110275

Lüdmann, T., Betzler, C., Eberli, G. P., Reolid, J., Reijmer, J. J., Sloss, C. R., et al. (2018). Carbonate delta drift: A new sediment drift type. *Mar. Geology* 401, 98–111. doi: 10.1016/j.margeo.2018.04.011

Lüdmann, T., Betzler, C., and Lindhorst, S. (2022). The Maldives, a key location of carbonate drifts. *Mar. Geology* 450, 106838. doi: 10.1016/j.margeo.2022.106838

Lüdmann, T., Kalvelage, C., Betzler, C., Fürstenau, J., and Hübscher, C. (2013). The Maldives, a giant isolated carbonate platform dominated by bottom currents. *Mar. Petroleum Geology* 43, 326–340. doi: 10.1016/j.marpetgeo.2013.01.004

Michel, J., Borgomano, J., and Reijmer, J. J. (2018). Heterozoan carbonates: When, where and why? A synthesis on parameters controlling carbonate production and occurrences. *Earth-Science Rev.* 182, 50–67. doi: 10.1016/j.earscirev.2018.05.003

Miller, K. G., Browning, J. V., Schmelz, W. J., Kopp, R. E., Mountain, G. S., and Wright, J. D. (2020). Cenozoic sea-level and cryospheric evolution from deep-sea geochemical and continental margin records. *Sci. Adv.* 6, 1–15. doi: 10.1126/sciadv.aaz1346

Montaggioni, L. F., Cabioch, G., Thouveny, N., Frank, N., Sato, T., and Sémah, A.-M. (2011). Revisiting the Quaternary development history of the western New Caledonian shelf system: from ramp to barrier reef. *Mar. Geology* 280, 57–75. doi: 10.1016/j.margeo.2010.12.001

Murray, R. W., and Leinen, M. (1996). Scavenged excess aluminum and its relationship to bulk titanium in biogenic sediment from the central equatorial Pacific Ocean. *Geochimica Et Cosmochimica Acta* 60, 3869–3878. doi: 10.1016/0016-7037(96)00236-0

Perea-Blázquez, A., Davy, S. K., and Bell, J. J. (2012). Nutrient utilisation by shallow water temperate sponges in New Zealand. Ancient Animals, New Challenges. *Hydrobiologia*, 687, 237–250. doi: 10.1007/s10750-011-0798-x

Principaud, M., Ponte, J. P., Mulder, T., Gillet, H., Robin, C., and Borgomano, J. (2016). Slope-to-basin stratigraphic evolution of the northwestern Great Bahama Bank (Bahamas) during the Neogene to Quaternary: Interactions between downslope and bottom currents deposits. *Basin Res.* 29, 699–724. doi: 10.1111/bre.12195

Purdy, E. G., and Bertram, G. T. (1993). Carbonate concepts from the Maldives, Indian ocean. *AAPG Stud. Geol.* 34, 1–56. doi: 10.1306/St34568

Reolid, J., Betzler, C., Braga, J. C., Lüdmann, T., Ling, A., and Eberli, G. P. (2020). Facies and geometry of drowning steps in a Miocene carbonate platform (Maldives). *Palaeogeography Palaeoclimatology Palaeoecol.* 538, 109455. doi: 10.1016/j.palaeo.2019.109455

Reolid, J., Betzler, C., and Lüdmann, T. (2019a). The record of Oligocene-Middle Miocene paleoenvironmental changes in a carbonate platform (IODP Exp. 359, Maldives, Indian Ocean). *Mar. Geology* 412, 199–216. doi: 10.1016/j.margeo.2019.03.011

Reolid, J., Betzler, C., and Lüdmann, T. (2019b). Facies and sedimentology of a carbonate delta drift (Miocene, Maldives). *Sedimentology* 66, 1243–1265. doi: 10.1111/sed.2019.66.issue-4

Reolid, J., Betzler, C., Singler, V., Stange, C., and Lindhorst, S. (2017). Facies variability in mixed carbonate–siliciclastic platform slopes (Miocene). *Facies* 63, 1–19. doi: 10.1007/s10347-016-0489-1

Sajid, Z., Ismail, M. S., Zakariah, M. N. A., Tsegab, H., Vintaned, J. A. G., Hanif., T., et al. (2020). Impact of paleosalinity, paleoredox, paleoproductivity/preservation on the organic matter enrichment in black shales from triassic turbidites of semanggol basin, peninsular Malaysia. *Minerals* 10, 1–34. doi: 10.3390/min10100915

Schlager, W. (2003). Benthic carbonate factories of the Phanerozoic. *Int. J. Earth Sci.* 92, 445–464. doi: 10.1007/s00531-003-0327-x

Schlager, W., Reijmer, J. J. G., and Droxler, A. (1994). Highstand shedding of carbonate platforms. *J. Sedimentary Res.* 64, 270–281. doi: 10.1306/D4267FAA-2B26-11D7-8648000102C1865D

Spezzaferri, S., Young, J., Stainbank, S., Coletti, G., and Kroon, D. (2022). Improved planktonic, benthic foraminiferal and nannofossil biostratigraphy aids the interpretation of the evolution at hole U1468A: IODP expedition 359, the Maldives. *Geosciences* 12, 239. doi: 10.3390/geosciences12060239

Steinbrink, L., Gohl, K., Riefstahl, F., Davy, B., and Carter, L. (2020). Late Cretaceous to recent ocean-bottom currents in the SW Pacific Gateway, southeastern Chatham Rise, New Zealand. *Palaeogeography Palaeoclimatology Palaeoecol.* 546, 109633. doi: 10.1016/j.palaeo.2020.109633

Swart, P. K. (2008). Global synchronous changes in the carbon isotopic composition of carbonate sediments unrelated to changes in the global carbon cycle. *Proc. Natl. Acad. Sci. United States America* 105, 13741–13745. doi: 10.1073/pnas.0802841105

Swart, P. K., and Eberli, G. (2005). The nature of the δ13C of periplatform sediments: Implications for stratigraphy and the global carbon cycle. *Sedimentary Geology* 175, 115–129. doi: 10.1016/j.sedgeo.2004.12.029

Swart, P. K., Mackenzie, G. J., Eberli, G. P., Lüdmann, T., and Betzler, C. (2019). Do drifts deposited adjacent to carbonate platforms record the signal of global carbon isotopic values? *Sedimentology* 66, 1410–1426. doi: 10.1111/sed.2019.66.issue-4

Tribovillard, N., Algeo, T. J., Lyons, T., and Riboulleau, A. (2006). Trace metals as paleoredox and paleoproductivity proxies: an update. *Chem. geology* 232, 12–32. doi: 10.1016/j.chemgeo.2006.02.012

Wang, D. S., Liu, Y., Zhang, J. C., Lang, Y., Li, Z., Tong, Z. Z., et al. (2022). Controls on marine primary productivity variation and organic matter accumulation during the Late Ordovician-Early Silurian transition. *Mar. Petroleum Geology* 142, 1–15. doi: 10.1016/j.marpetgeo.2022.105742

Westerhold, T., Marwan, N., Drury, A. J., Liebrand, D., Agnini, C., Anagnostou, E., et al. (2020). An astronomically dated record of Earth's climate and its predictability over the last 66 million years. *Science* 369, 1383–1387. doi: 10.1126/science.aba6853

Wu, F., Xie, X. N., Betzler, C., Zhu, W. L., Zhu, Y. H., Guo, L. Y., et al. (2019b). The impact of eustatic sea-level fluctuations, temperature variations and nutrient-level changes since the Pliocene on tropical carbonate platform (Xisha Islands, South China Sea). *Palaeogeogr. Palaeoclimatol. Palaeoecol.* 514, 373–385. doi: 10.1016/j.palaeo.2018.10.013

Wu, F., Xie, X., Coletti, G., Zhu, Y., Chen, B., and Shang, Z. (2023). Coralline algal and foraminiferal records of the Pliocene paleoclimatic conditions and water-depth changes in the northern South China Sea. *Mar. Petroleum Geology* 153, 106276. doi: 10.1016/j.marpetgeo.2023.106276

Wu, F., Xie, X. N., Li, X. S., Betzler, C., Shang, Z., and Cui, Y. (2019a). Carbonate factory turnovers influenced by the monsoon (Xisha Islands, South China Sea). *J. Geological Soc.* 176, 885–897. doi: 10.1144/jgs2018-086

Wu, F., Xie, X. N., Zhu, Y. H., Coletti, G., Betzler, C., Cui, Y. C., et al. (2021). Early development of carbonate platform (Xisha Islands) in the northern South China Sea. *Mar. Geology* 441, 1–16. doi: 10.1016/j.margeo.2021.106629

Wunsch, M., Betzler, C., Eberli, G. P., Lindhorst, S., Lüdmann, T., and Reijmer, J. J. G. (2018). Sedimentary dynamics and high-frequency sequence stratigraphy of the southwestern slope of Great Bahama Bank. *Sedimentary Geology* 363, 96–117. doi: 10.1016/j.sedgeo.2017.10.013